Structural, Bonding, and Electrochemical Properties of Perfluorinated Fullerene C_{70}

Daniel Claves,* Jérôme Giraudet, and André Hamwi

Laboratoire des Matériaux Inorganiques, Université Blaise Pascal, UPRES CNRS No. 6002 24, Av. des Landais, 63177 Aubière Cedex, France

Roland Benoit

Centre de Recherche sur la Matière Divisée—CNRS, 1 Rue de la Férollerie, 45071 Orléans Cedex, France

Received: July 24, 2000; In Final Form: November 28, 2000

The synthesis of a perfluorinated compound of average composition $C_{70}F_{56}$ is described. The associated properties are examined at the molecular level and for the bulk material. It is shown that fluorination involves an expansion of the carbon frame and that the length of the resulting C−F bond is elongated to 1.45 Å and possesses an ionocovalent nature. The corresponding crystalline product has fcc symmetry related to complete orientational disorder of the fluorinated molecules. When $C_{70}F_{56}$ is used in lithium batteries, the formation of LiF results via a preliminary intercalation reaction.

1. Introduction

Fluorinated fullerenes present important potential as molecular materials with oxidizing properties and tunable π-electron densities.

The fluorination rate of fullerene C_{60} under a F_2 atmosphere strongly depends on the thermal conditions used, for a given reaction time. Whereas polyfluorinated $C_{60}F_x$ molecules with moderate fluorine contents are obtained at low temperatures,[1−5] highly fluorinated products with a narrow distribution in composition form at elevated temperatures.[3,5−8] Studies performed on pure C_{70} remain scarce but seem to reach the same conclusion, as reported earlier from results on C_{60}/C_{70} mixtures[1,3,6] or in more recent works.[4,8]

From a structural point of view, samples of sublimed or high-temperature-prepared fluorofullerenes $C_{60}F_x$ with reduced ranges of mass distribution were respectively shown to consist in a mixture of fcc and hcp phases[2,5] for an average value of x near 40 or in a single fcc phase[5] for x near 50. The crystal lattices of pure $C_{60}F_{36}$ and $C_{60}F_{48}$ were recently found to be of the bcc and bct types, respectively.[9] A phase transition toward fcc packing was observed at high temperature for the latter.

The electrochemistry of fluorofullerenes strongly reflects their oxidizing character. Thus, in solution, shifts near 1−1.5 V toward positive potentials were observed for the first reduction wave, compared to the unfluorinated molecules.[10−13] So far, their performances as cathode materials have remained limited, exhibiting a dependence of the capacity and open circuit voltage (OCV) on the fluorine content, and irreversible reduction steps due to the formation of LiF.[14]

In this paper, we give a detailed description of the synthesis and solid-state properties, including structural characterization, of a nearly homogeneous (not a single compound, however) perfluorinated C_{70} material. We show that when this material is used in lithium cell batteries, a capacity of up to several hundreds of $mA{\cdot}h{\cdot}g^{-1}$ can be obtained. The resulting electrochemical process can be decomposed into different steps.

2. Experimental Section

The fluorination reaction of finely ground C_{70} powders was carried out at 300 °C under fluorine gas flow in a tubular Monel reactor. After 3 h, a white compound was obtained.

X-ray diffraction data were collected from a D-501 Siemens diffractometer, using conventional Bragg−Brentano geometry and Cu Kα radiation.

The composition of the samples and the characteristics of the C−F bonds were established by FTIR and core level photoelectron spectroscopy. The XPS analyses were performed with an Escalab MK II multidetection spectrometer. Nonmonochromatic Mg Kα radiation (1253.6 eV, 200 W) was used. The binding energies were referenced to the Au $4f_{7/2}$ core level of gold deposited on the sample.

Fluorinated samples were tested as cathode materials in lithium batteries under the form of composite mixtures with graphite (30 wt %) or carbon black (10 wt %) embeded in a $(PEO)_8LiClO_4$ ionically conducting interface (∼30 wt %). A lithium disk was used as the negative electrode. The electrolyte medium was a $(PEO)_8LiClO_4$ film. The latter solid-state cells were operated at 80 °C. Electrochemical studies were performed by means of galvanostatic charge/discharge and cyclic voltammetry.

3. Bonding

The average elemental composition determined by XPS is $C_{70}F_{56}$. The fluorine content was established from the ratio of the integrated C_{1s} and F_{1s} peak areas. No evidence for oxygenated adducts was revealed up to the detection threshold of the spectrometer. It was carefully checked that no degradation of the sample occurred upon irradiation, on the time scale of the experiment.

Regardless of the fine structure, the XPS spectra[15−17] of pure C_{60} and C_{70} exhibit a single peak centered near 285 eV, whereas the C_{1s} spectrum (Figure 1) of $C_{70}F_{56}$ comprises two main features shifted toward higher energies. Such splitting and shifts of the C_{1s} core level energy with fluorine addition have been

10.1021/jp0026336 CCC: $20.00
Published on Web 02/10/2001

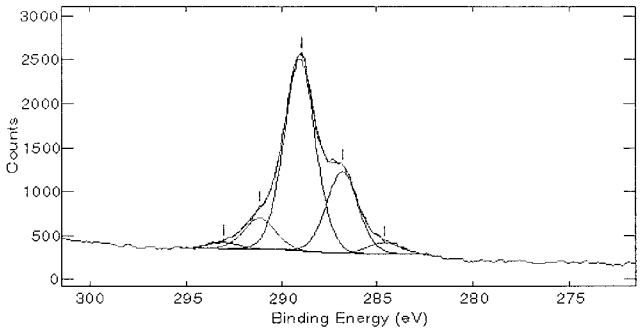

Figure 1. C_{1s} XPS spectrum of high-temperature fluorinated C_{70}.

TABLE 1: C_{1s} XPS Data from $C_{70}F_{56}$[a]

C_{1s} binding energy (eV)	atom	intensity
284.6	bare C	2.9
286.8	bare C with fluorinated neighbors	25.6
289.1	monosubstituted C	60.1
291.2	disubstituted C	9.7
293.1	disubstituted C with neighboring disubstituted C, or trisubstituted C	1.7

[a] The composition established from the peak assignment is in fair agreement with the one obtained from the F/C area ratio.

reported previously for covalent graphite fluoride $(C_2F)_n$[18] and for many $C_{60}F_x$ compounds,[19−22] and it was shown that the binding energy of fluorinated carbon atoms is higher than that of unsubstituted carbon atoms whose nearest neighbor is directly bonded to fluorine. The remaining part of the C_{1s} signal at the lowest and highest energies can be attributed to bare carbons and $>CF_2$ groups, respectively, showing that some fullerene molecules begin to undergo cage rupture under these conditions. This suggests that the F/C = 0.8 ratio obtained represents the upper limit of fluorination before unstability begins to manifest. It is worth noting that an exactly identical value of the critical ratio was deduced in the case of the fluorination of C_{60}, since $C_{60}F_{48}$ is known as the highest fluorinated product easily isolable, partial opening of the carbon shell occurring most of the time upon further fluorination.[6−8] The F_{1s} spectrum is characteristic of F atoms in an essentially single environment and presents a single peak centered at 688.1 eV. This value is slightly inferior to the binding energy of F atoms involved in purely covalent alternating C−F groups[18,23,24] (F_{1s} signals of covalent graphite fluorides, C_6F_6, PTFE, fall in the range 689−691 eV) but is well above the level of purely ionic fluorides[25,26] (683−685 eV) and reflects the intermediate character of the C−F bond in our compound. XPS data are summarized in Table 1.

Whereas polyfluorinated $C_{60}F_x$ compounds gave broad IR absorption bands[1,6,8] centered around 1150 cm^{-1}, the relatively well resolved bands observed here (Figure 2) reflect the presence of a reduced number of components (composition, isomers) in our sample, but though certainly restricted a mass distribution remains highly probable.

The infrared spectrum of $C_{70}F_{56}$ exhibits an intense line centered at 1138 cm^{-1}, downshifted in regard to the position of the C−F stretching bands of covalent graphite fluorides $(C_xF)_n$ (x = 1, 2), which usually appear in the 1215−1220 cm^{-1} region.[18,27,28] This behavior reveals a weaker bond strength and is consistent with the appearance of partial ionic character, since the same effect, with comparable amplitude, was reported[28−31] in the case of semiionic graphite fluorides C_xF. The absence of any −OH group signature in the high-wavenumber region of the spectrum confirms the stability of such products toward hydrolysis upon air exposure.

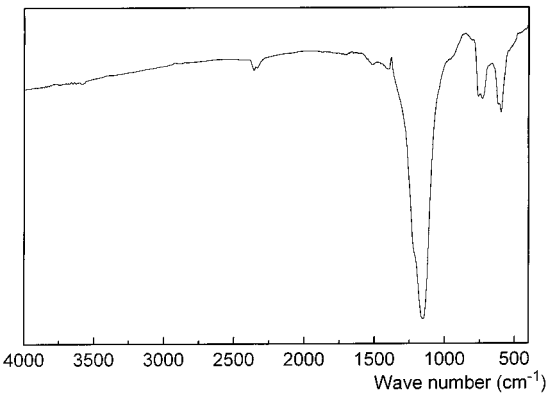

Figure 2. FTIR spectrum of high-temperature fluorinated C_{70}.

4. Structure

The diffraction pattern is composed of thin peaks, which confirm a narrow distribution in composition, as obtained earlier from $C_{60}F_x$ samples with a unique composition[9] or through distillation of polyfluorinated products.[2,5] All reflections can be assigned indices characterizing fcc symmetry. The occurrence of a high crystal symmetry necessarily implies the presence of randomly oriented molecules in the lattice to account for the lower D_{5h}-derived point symmetry of the fluorinated molecules. Thus, complete orientational disorder raises the apparent symmetry to $Fm\bar{3}m$. Additional features in the pattern, such as the shoulder on the cubic (111) reflection and the emergence of a broad line in the (220)−(311) region, were tentatively interpreted as (100) and (103) peaks from a coexisting hcp structure. Kniaz et al. showed earlier[2] that highly fluorinated C_{60} can indeed consist in a mixture of two such phases. Somehow, in the present case, the admixture of a hexagonal phase could be ruled out from the absence of the usually strong (101) reflection characterizing hexagonal close-packing, and the above-mentioned features have to be related to growth faults in a cubic structure. Extended cubic ABCABC stacked regions are well-known to frequently alternate with hexagonal ABAB sequences, producing stacking disorder. Vaughan et al. showed[32] that strictly identical and typical sawtooth foot and broad peak appear in the same regions of the diffraction pattern of pure C_{60}, when the lattice contains some quantity of stacking faults.

A Rietveld refinement was performed on the assumption that the inner carbon skeleton is constrained to D_{5h} molecular symmetry as in the unfluorinated material. The global structural model includes a spherically averaged molecular form factor, which is the Fourier transform of concentric spheres with uniform surface electron densities, centered at lattice sites:

$$f_{C70\,Fx}(Q) = f_C \sum_{i=1}^{5} N_i \sin(QR_i)/QR_i + \frac{x}{70} f_F \sum_{i=1}^{5} N_i \sin[Q(R_i + L_{C-F})]/Q(R_i + L_{C-F})$$

where the fluorine content x, the carbon−fluorine bond length L_{C-F}, and the carbon sphere radii are refinable parameters, f_C and f_F are the carbon and fluorine atomic form factors, N_i is the number of carbon atoms at distance R_i from the center of the molecule, and Q is the amplitude of the scattering vector. The N_i and initial R_i values used in the present calculations are

TABLE 2: Axial Distribution (N_i) of Carbon Atoms along Rings and Their Distance R_i (from Ref 33) to the Center of the Molecule[a]

N_i (no. of C atoms)	R_i (Å)	N_i (no. of C atoms)	R_i (Å)	N_i (no. of C atoms)	R_i (Å)
10	3.565	20	3.876	10	4.172
20	3.663	10	4.029		

[a] The long axis of the rugby-ball-shaped C_{70} molecule is set vertically.

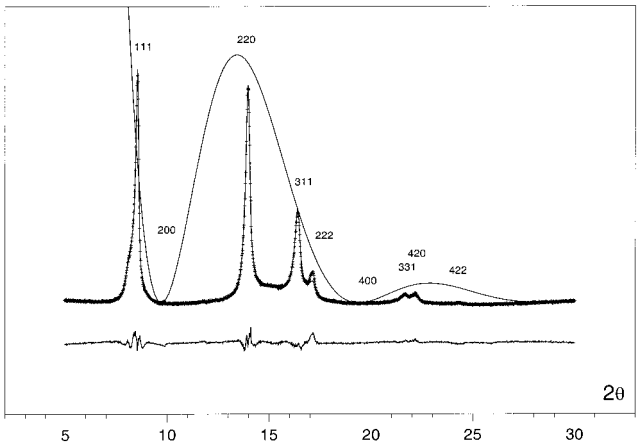

Figure 3. Rietveld refinement (R_{wp}= 0.118), using a random orientation model, of powder diffraction data obtained from $C_{70}F_{56}$. Bottom: difference plot. The square of the value taken by the spherical molecular form factor in each angular zone has been superimposed to the diffraction profile. The vanishing of (200) and (400) lines comes from waves scattered by the carbon and fluorine shells, opposed in phase.

summarized in Table 2. We modeled the intensity distribution due to stacking disorder by the introduction into the refinement procedure of two additional and essentially Gaussian line shapes with adjustable parameters, beside the unfaulted fcc structure. To avoid self-compensating parameters, it happened to be necessary to hold the average composition of the sample fixed, according to the fluorine content obtained by XPS.

We first assumed that no perturbation of the carbon atomic positions was induced, despite reinforcement of the sp^3 character of the inner frame upon fluorination. Such a model led to a bad agreement in regard to the intensities of the (111) and (311) lines. An analysis of the separate influence of the superimposed carbon shells or fluorine shells, on the intensity of a given reflection, showed that the part of the molecular form factor due to fluorine falls to nearly zero in the (111) and (311)−(222) regions and that consequently only carbon atoms contribute to these reflections. This suggests that the above-mentioned difference in the observed and calculated intensities for these lines may find its origin in inappropriate atomic parameters for carbon atoms. In the last step of the refinement, the latter were then allowed to move radially to check whether fluorination could result in an inflation, considered isotropic, of the carbon cage. A significant improvement of the fit was obtained on the basis of such a model, and an average 0.1 ± 0.03 Å expansion of the inner frame was determined. The global results were then consistent with a model of close-packed spheres, homogeneous in size. The cell parameter was refined to 17.949(5) Å, and the C−F bond length allowing the best fit to experimental data was 1.45 ± 0.03 Å. Due to steric hindrance between fluorine atoms at the surface of the molecule, it appears much longer than the usual 1.35 ± 0.03 Å distance usually observed in fluoroalkanes and is consistent with a reduced covalent character of the C−F bond, in agreement with the conclusions of the above XPS and IR studies. A similar value

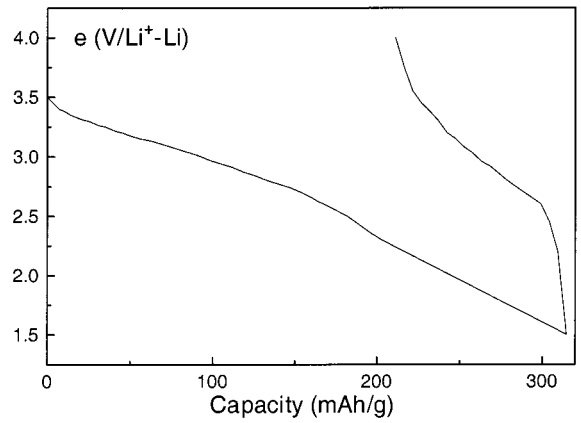

Figure 4. Galvanostatic discharge/charge characteristics, under 10 μA, of a $C_{70}F_{56}$-based primary lithium battery.

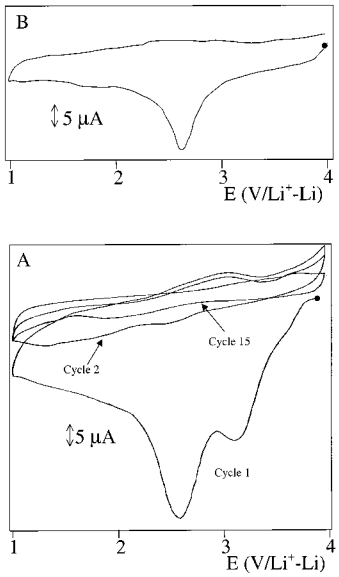

Figure 5. Cyclic voltammetry at 15 mV/min (A) and 1.5 mV/min (B) of the $C_{70}F_{56}$/Li system.

of 1.49 Å was reported[2] in the case of highly fluorinated C_{60}. As shown in Figure 3, the refined profile closely matches the experimental pattern, though the amplitude of the (222) line remains underestimated.

The accuracy of the bond lengths determined is however limited by compensating effects between the two refined distances. We also infer that the discrepancy between the observed and calculated intensities of the (222) reflection may arise from those fluorine atoms, irregularly distributed between the averaged spherical layers, which appear when some C−C bonds are broken. These additional electron density regions should induce some perturbations in the molecular form factor.

5. Electrochemical Properties

The fluorinated product was tested as a positive electrode material in lithium batteries, using solid-state cells, according to the conditions described in the Experimental Section.

Figure 4 displays the electrochemical behavior of the system under galvanostatic charge/discharge conditions. The high value of the OCV reflects the highly oxidizing properties of the fluorinated molecules due to the strong electron-withdrawing character of fluorine and to the emergence of deeper π-levels after the addition reaction. The curves show a continuous reduction of $C_{70}F_{56}$ and the absence of a corresponding

reoxidation process. The gradual decrease of the discharge potential represents an intermediate behavior between the regular plateaus characterizing intercalation into well-ordered materials and the rapid voltage dropping characterizing intercalation into disordered phases. Such discharge characteristics should be attributed to the presence, in the semicrystalline material under study, of interstitial sites at different chemical potential values, since the random distribution of orientations of the fluorinated molecules in the crystal excludes the opportunity of a regular local symmetry at each lattice site. The discharge process should therefore result in the formation, via electrochemical doping by Li^+ cations, of $Li_xC_{70}F_{56}$ phases. It seems very likely that the latter are unstable and rapidly turn into LiF, conferring the system its important irreversible capacity.

Cyclic voltammetry (Figure 5) allows a complementary picture of the reduction process through the distinction of successive irreversible and ill-defined reduction steps, which may be attributed to the continuous accommodation of Li^+ cations in the pristine and in the reduced lattice, according to different schemes:

$$C_{70}F_{56} + xLi^+ + xe^- \rightarrow Li_xC_{70}F_{56} \rightarrow C_{70}F_{56-x} + xLiF$$

$$Li_xC_{70}F_{56} + yLi^+ + ye^- \rightarrow Li_{x+y}C_{70}F_{56} \rightarrow C_{70}F_{56-x-y} + (x+y)LiF$$

$$C_{70}F_{56-x} + zLi^+ + ze^- \rightarrow Li_zC_{70}F_{56-x} \rightarrow C_{70}F_{56-x-z} + zLiF$$

(... and so on)

The global result is an indirect reduction of the C−F bond and a gradual loss of fluorine. The higher the fluorine content is, the faster decomposition of the intercalated phase into LiF seems to occur, since the low potential reduction steps appear partly reversible on the time scale of the experiment. If the sweep rate is sufficiently slow (Figure 5B), all reversibility is lost. Our conclusions do not differ significantly from those of Liu et al.[14] in their earlier cyclic voltammetry study of polydispersed fluorofullerene samples with a lower fluorine content.

6. Conclusion

The high-temperature fluorination of fullerene C_{70} yields highly fluorinated molecules with a narrow dispersion of the F/C ratio. A temperature of 300 °C seems to be the highest conceivable temperature in the synthesis process, cage rupture being highly probable to occur above this limit. This fact strongly compromises the eventuality of the synthesis of a completely fluorinated C_{70} molecule. The nature of the C−F bond in the material prepared at 300 °C was found to be semiionic. Fluorination induces an absence of true long-range order in the solid, due to random orientational disorder of the molecules. The electrochemical performances of such kinds of materials remain limited, from a practical point of view, by an essentially low potential (<3 V vs Li^+/Li) discharge capacity.

References and Notes

(1) Selig, H.; Lifshitz, C.; Peres, T.; Fisher, J. E.; McGhie, A. R.; Romanow, W. J.; McCauley, J. P., Jr.; Smith, A. B., III. *J. Am. Chem. Soc.* **1991**, *113*, 5475.

(2) Kniaz, K.; Fisher, J. E.; Selig, H.; Vaughan, G. B. M.; Romanow, W. J.; Cox, D. M.; Chowdhury, S. K.; McCauley, J. P.; Strongin, R. M.; Smith, A. B., III. *J. Am. Chem. Soc.* **1993**, *115*, (14), 6060.

(3) Hamwi, A.; Fabre, C.; Chaurand, P.; Della-Negra, S.; Ciot, C.; Djurado, D.; Dupuis, J.; Rassat, R. *Fullerene Sci. Technol.* **1993**, *1*, 499.

(4) Taylor, R.; Langley, G. J.; Holloway, J. H.; Hope, E. G.; Brisdon, A. K.; Kroto, H. W.; Walton, D. R. M. *J. Chem. Soc., Perkin Trans. 2* **1995**, 181.

(5) Hamwi, A.; Latouche, C.; Marchand, V.; Dupuis, J.; Benoit, R. *J. Phys. Chem. Solids* **1996**, 991.

(6) Tuinman, A. A.; Mukherjee, P.; Adcock, J. L.; Hettich, R. L.; Compton, R. L. *J. Phys. Chem.* **1992**, *96*, 7584.

(7) Gakh, A. A.; Tuinman, A. A.; Adcock, J. L.; Sachleben, R. A.; Compton, R. N. *J. Am. Chem. Soc.* **1994**, *116*, 819.

(8) Boltalina, O. V.; Sidorov, L. N.; Bagryantsev, V. F.; Seredenko, V. A.; Zapol'skii, A. S.; Street, J. M.; Taylor, R. *J. Chem. Soc., Perkin Trans. 2* **1996**, 2275.

(9) Kawasaki, S.; Aketa, T.; Touhara, H.; Okino, F.; Boltalina, O. V.; Gol'dt, I. V.; Troyanov, S. I.; Taylor, R. *J. Phys. Chem. B* **1999**, *103*, 1223.

(10) Zhou, F.; Van Berkel, G. J.; Donovan, B. *J. Am. Chem. Soc.* **1994**, *116* (12), 5485.

(11) Okino, F.; Yajima, S.; Suganuma, S.; Mitsumoto, R.; Seki, K.; Touhara, H. *Synth. Met.* **1995**, *70*, 1447.

(12) Liu, N.; Touhara, H.; Morio, Y.; Komichi, D.; Okino, F.; Kawasaki, S. *J. Electrochem. Soc.* **1996**, *143* (9), L-214.

(13) Liu, N.; Morio, Y.; Okino, F.; Touhara, H.; Boltalina, O. V.; Pavlovich, V. K. *Synth. Met.* **1997**, *86*, 2289.

(14) Liu, N.; Touhara, H.; Okino, F.; Kawasaki, S.; Nakacho, Y. *J. Electrochem. Soc.* **1996**, *143* (7), 2267.

(15) Weaver, J. H.; Martins, J. L.; Komeda, T.; Chen, Y.; Ohno, T. R.; Kroll, G. H.; Troullier, N.; Haufler, R. E.; Smalley, R. E. *Phys. Rev. Lett.* **1991**, *66*, 1741.

(16) Benning, P. J.; Poirier, D. M.; Ohno, T. R.; Chen, Y.; Jost, M. B.; Stepniak, F.; Kroll, G. H.; Weaver, J. H.; Fure, J.; Smalley, R. E. *Phys. Rev. B* **1992**, *45*, 6899.

(17) Han, B.; Yu, L.; Hevesi, K.; Gensterblum, G.; Rudolf, P.; Pireaux, J. J.; Thiry, P. A.; Caudano, R.; Lambin, Ph.; Lucas, A. A. *Phys. Rev. B* **1995**, *51*, 7179.

(18) Kita, Y.; Watanabe, N.; Fujii, Y. *J. Am. Chem. Soc.* **1979**, *101* (14), 3832.

(19) Benning, P. J.; Ohno, T. R.; Weaver, J. H.; Mukherjee, P.; Adcock, J. L.; Compton, R. N.; Dunlap, B. I. *Phys. Rev. B* **1993**, *47* (3), 1589.

(20) Cox, D. M.; Cameron, S. D.; Tuinman, A.; Gakh, A.; Adcock, J. L.; Compton, R. N.; Hagaman, E. W.; Kniaz, K.; Fisher, J. E.; Strongin, R. M.; Cichy, M. A.; Smith, A. B., III. *J. Am. Chem. Soc.* **1994**, *116*, 1115.

(21) Matsuo, Y.; Nakajima, T.; Kasamatsu, S. *J. Fluorine Chem.* **1996**, *78*, 7.

(22) Mitsumoto, R.; Araki, T.; Ito, E.; Ouchi, Y.; Seki, K.; Kikuchi, K.; Achiba, Y.; Kurosaki, H.; Sonoda, T.; Kobayashi, H.; Boltalina, O. V.; Pavlovich, K.; Sidorov, L. N.; Hattori, Y.; Liu, N.; Yajima, S.; Kawasaki, S.; Okino, F.; Touhara, H. *J. Phys. Chem. A* **1998**, *102* (3), 552.

(23) Nansé, G.; Papirer, E.; Fioux, P.; Moguet, F.; Tressaud, A. *Carbon* **1997**, *35* (2), 175.

(24) Briggs, D.; Seah, M. P. *Practical Surface Analysis*, 2nd ed.; J. Wiley & Sons: New York, 1993; Vol. 1.

(25) Nefedov, V. I.; Gati, D.; Dzhurinskii, B. F.; Sergushin, N. P.; Salyn, Y. V. *Russ. J. Inorg. Chem.* **1975**, *20*, 1279.

(26) Wagner, C. D.; Riggs, W. M.; Davis, L. E.; Moulder, J. F. *Handbook of X-ray Photoelectron Spectroscopy*; Perkin-Elmer Corp., Physical Electronics Division.

(27) Rüdorff, W.; Brodersen, K. *Z. Naturforsch., B* **1957**, *126*, 595.

(28) Lagow, R. J.; Badachhape, R. B.; Wood, J. L.; Margrave, J. L. *J. Chem. Soc., Dalton Trans.* **1974**, 1268.

(29) Mallouk, T.; Bartlett, N. *J. Chem. Soc., Chem. Commun.* **1983**, 103.

(30) Hamwi, A.; Daoud, M.; Cousseins, J. C. *Synth. Met.* **1988**, *26*, 89.

(31) Hagiwara, R.; Lerner, M.; Bartlett, N. *J. Chem. Soc., Chem. Commun.* **1989**, 573.

(32) Vaughan, G. B. M.; Chabre, Y.; Dubois, D. *Europhys. Lett.* **1995**, *31* (9), 525.

(33) Baker, J.; Fowler, P. W.; Lazzaretti, P.; Malagoli, M.; Zanasi, R. *Chem. Phys. Lett.* **1991**, *184* (1−3), 182.